



## Research Article

# Controlled release of metformin-loaded SA/PEG scaffolds produced by 3d-printing technology

Sena HARMANCI<sup>1,2</sup>, Sümeyye CESUR<sup>1</sup>, Oğuzhan GÜNDÜZ<sup>1,3</sup>, Cem Bülent ÜSTÜNDAĞ<sup>2,\*</sup>

<sup>1</sup>Center for Nanotechnology & Biomaterials Application and Research (NBUAM), Marmara University, 34722, Türkiye

<sup>2</sup>Department of Bioengineering, Faculty of Chemical and Metallurgical Engineering, Yıldız Technical University, 34220, Türkiye

<sup>3</sup>Department of Metallurgical and Materials Engineering, Faculty of Technology, Marmara University, 34722, Türkiye

## ARTICLE INFO

### Article history

Received: 03 November 2021

Revised: 19 November 2021

Accepted: 23 March 2022

### Keywords:

3D Printing; Drug Release;  
Metformin; Diabetes Mellitus

## ABSTRACT

Type 2 diabetes mellitus (T2DM) is a long-term metabolic disease that is commonly characterized by insulin deficiency or resistance, and prevalence has been increasing gradually all over the world. The aim of this study is to produce Metformin-loaded 3D printed scaffolds for an alternative drug delivery application in the treatment of Type 2 DM with two different biopolymers. Sodium Alginate (SA)/Polyethylene glycol (PEG) scaffolds loaded with varying concentrations of Metformin (0.5 and 2 wt.%) were prepared by adding 9 wt.% of SA to 3 wt.% of PEG. The physical analyses of the solutions were examined after the production process, and as a result, no significant changes were observed in the viscosity, density, and surface tension of the solutions with the addition of Metformin. Morphological (SEM), molecular interaction (FTIR), thermal analysis (DSC), tensile strength analyses were done. SEM images and histograms showed that the desired pore structure was obtained in the scaffolds produced by the 3D printing method, and the average pore sizes were  $236.14 \pm 18.999$ ,  $255.28 \pm 14.168$ , and  $318.83 \pm 13.038$   $\mu\text{m}$  for SA/PEG, 0.5% and 2% Metformin-loaded scaffolds, respectively. A drug release test was performed by UV spectroscopy. Metformin from both 0.5% and 2% scaffolds showed a burst release in 30 minutes because of the high solubility of SA and PEG in water. More than 97% of the drug was released from both scaffolds. However, they displayed sustained release up to 24 hours. Therefore, Metformin-loaded 3D-printed scaffolds have promising potential for the treatment of T2DM as they are an alternative to the oral administration of the drug.

**Cite this article as:** Harmancı S, Cesur S, Gündüz O, Üstündağ CB. Controlled release of metformin-loaded SA/PEG scaffolds produced by 3d-printing technology. Sigma J Eng Nat Sci 2023;41(6):1106–1114.

## INTRODUCTION

Type 2 Diabetes Mellitus (T2DM) is a chronic disease that occurs because of the dysfunction of  $\beta$ -cells

in the pancreas, resulting in impaired insulin resistance and insulin secretion in the body [1]. According to 2019 data from the International Diabetes Federation 9.3% of adults aged between 20–79, nearly 463 million people, are

### \*Corresponding author.

\*E-mail address: [cbustundag@gmail.com](mailto:cbustundag@gmail.com)

This paper was recommended for publication in revised form by Regional Editor Hakan Yilmazer



suffering from diabetes [2]. Oral antidiabetic drugs such as Metformin, sulfonylureas (SU), and thiazolidinediones (TZD) have been used for the treatment of T2DM as they provide better glycaemic control [3,4]. However, Metformin is accepted as first-line therapy due to its good safety profile, improved glycaemic control without the hypoglycemia risk, and low cost [5]. Metformin is a biguanide derivative that works as an insulin sensitizer by acting on insulin resistance. Metformin is an orally administered, low bioavailable, and not metabolized drug [5]. The half-life ( $t_{1/2}$ ) of the drug is between 2-5 hours in patients with normal renal function, and nearly 90% of the drug is eliminated in 12 hours [6]. Metformin has no serious side effects, but drug overdose can cause lactic acidosis, especially in people with certain medical conditions [7]. Several drug delivery systems have been designed to increase the bioavailability and effect of orally administered antidiabetic drugs [8].

3D printed scaffolds are used in many areas due to their advantages, such as fast and low-cost production [9]. Scaffolds can produce from different materials with different porosities and pore sizes. They are biocompatible, and also can show structural and mechanical similarities with the host tissues [10]. Extrusion-based 3D printing systems are used computer-aided design (CAD) files to fabricate scaffolds [11]. This method has so much potential due to low cost, diversity with the design, and material selection [12]. The 3D printing method allows the production of tissue scaffolds with different drug release profiles in various geometries and designs [13]. Natural and synthetic polymers and their composites can be used to manufacture 3D scaffolds [14].

Sodium Alginate (SA) is a natural polymer consisting of  $\beta$  (1-4) linked D-mannuronic acid (M), and  $\alpha$  (1-4) linked L-guluronic acid (G) units [15]. SA is a water-soluble polysaccharide mostly obtained from brown algae. It is commonly used in tissue engineering applications due to the advantages of its non-toxicity, biodegradability, and biocompatibility [16]. SA shows good swelling behaviour, but this also causes deformation of the material easily. To prevent this SA can be blended with natural and synthetic polymers such as collagen, gelatin, elastin, chitosan, polyacrylamide, polystyrene, polyurethane, polyvinyl alcohol, and polyethylene glycol [15]. PEG is a synthetic and hydrophilic polymer used in biomedical applications [17]. PEG addition to the polymer solution can help to control the degradation [18]. PEG's favorite properties are non-toxicity and biocompatibility [19]. In previous studies, Metformin has been produced with other oral antidiabetics or as a stand-alone oral dosage form. The fused deposition modeling (FDM) method and thermoplastic polymers have been widely used.

In this study, biocompatible, biodegradable, and non-toxic 3D scaffolds were designed and produced as an alternative route to oral administration of Metformin. Transdermal drug delivery systems can increase the efficiency and bioavailability of Metformin, which is used as a

first-line drug in the treatment of type 2 diabetes. Due to the widespread use of SA and PEG polymers in drug delivery systems, the scaffolds were produced with these polymers.

## MATERIALS AND METHODS

### Materials

Poly (ethylene glycol) (PEG, MW:4000 g/mol), Sodium alginate (SA, MW:216000 g/mol), and dimethyl sulfoxide (DMSO) were provided from Sigma-Aldrich. Calcium chloride ( $\text{CaCl}_2$ ) was bought from Yasin Teknik Company. Metformin was obtained as a powder form from Sigma-Aldrich, USA.

### Methods

#### Preparation of the polymer solutions

PEG/SA solutions with diverse Metformin concentrations were prepared. SA solution was dissolved in 10 mL distilled water at 9% (w/v). It was stirred at room temperature for about 1 hour using a magnetic stirrer (WiseStir®, MSH-20A, Germany). After that, PEG was dissolved in 10 mL distilled water at 3% (w/v). The solution was stirred for 20 minutes. Subsequently, PEG and SA solutions were formed in different beakers, and mixed in a 5:1 ratio, respectively. To obtain the final SA/PEG solution, the mixture was stirred for 30 minutes using a magnetic stirrer. When the SA/PEG mixture was optimized, Metformin was added to the solution and prepared in the same conditions. The drug was dissolved in distilled water with PEG and mixed with SA. 0.5 and 2% (w/v) Metformin were added into the 6 mL SA/PEG solutions. After that, the solutions were stirred well at room temperature and prepared for printing.

#### Design and production of the 3d printed scaffolds

The printing process of the scaffolds was carried out with an extrusion 3D printer (Hyrel 3D, SDS-5 Extruder, GA, USA). Firstly, scaffolds were designed using Solidworks, a 3D drawing program, and it was converted to G-codes by Simplify 3D slicing software. The scaffolds were designed to be square, and their dimensions were 20 mm x 20 mm x 1 mm. Then, a 10 mL syringe directly connected to the needle tip (25 Ga) was filled with the prepared polymer solution. The printing parameters were adjusted for each scaffold such that the fill density was 96%, the total layer 7, and the fill pattern was rectilinear. During the printing process, the flow rate was 1 mL/h and the printing rate 10 mm/s. Lastly, all scaffolds were sprayed with  $\text{CaCl}_2$  solution for 5 minutes for crosslinking.

#### Characterization of physical properties of the solutions

The physical properties of the polymer solutions, such as density, surface tension, and viscosity, were analysed. The density of the polymer solutions was investigated using DIN ISO 3507-Gay-Lussac (Boru Cam Inc., Republic of Turkey) with a 10 mL standard density bottle. The surface

tension was measured with a force tensiometer (Sigma 703D, Attention, Germany), and the viscosity of the polymer solutions was determined by using a digital viscometer (DV-E, Brookfield AMETEK, USA). Both analyses were carried out at room temperature. Each test was performed 3 times. Also, each piece of equipment used in the analyses was calibrated beforehand.

#### Fourier transform infrared spectroscopy analyses

Fourier transform infrared spectroscopy (FTIR) (Jasco, FT/IR 4700) was used to identify the chemical interactions and molecular structures in the scaffolds. Analysis was performed in transmission mode, and the wavelength ranged between 450 and 4000  $\text{cm}^{-1}$ .

#### Thermal analysis of the scaffolds

The thermal properties such as glass transition and the melting temperature of the scaffolds were characterized with a differential scanning calorimetry (DSC) (Shimadzu, Japan) in the closed pan. During the process, the temperature ranged from 25–400  $^{\circ}\text{C}$ , and the heating rate was set to 10  $^{\circ}\text{C}/\text{min}$ . Inert nitrogen gas was used as purge gas at a flow rate of 25  $\text{mL}/\text{min}$ .

#### Scanning electron microscopy (SEM)

The pore sizes and the surface morphologies of the 3D printed scaffolds were investigated with Scanning Electron Microscopy (EVA MA 10, ZEISS, USA). Before the process, the scaffolds were coated with gold (Au) for 120 seconds with a sputter coating machine (Quorum SC7620, ABD). Measurements of the pore sizes were done with Analysis5, Olympus (USA) software, and for each scaffold, the pore sizes were adjusted.

#### Mechanical properties of the scaffolds

A tensile test machine (SHIMADZU, EZ-LX, China) was used to measure the tensile strength of the scaffolds. Before the test, each scaffold was fully dried. The tensile test was done in which the upper and lower sides of each sample were located horizontally in the respective part of the device.

#### Drug release study

At first, Metformin was prepared in 6 different concentrations (4, 6, 8, 10, 12, and 14  $\mu\text{g}/\text{mL}$ ) to draw a calibration curve. Release kinetics of scaffolds with different Metformin (0.5 and 2 wt. %) ratios were analysed. Firstly, the scaffolds were weighted, then put in different Eppendorf tubes, and

1 mL of PBS solution (pH 7.4 at 37  $^{\circ}\text{C}$ ) was added to the tubes. The test was performed in a shaking incubator (37  $^{\circ}\text{C}$ , 200 rpm) for 24 hours. 1 mL of the solution was taken from the tubes at different time periods, and to measure the released drug amount, the solution was analysed in a UV-vis spectrophotometer (Shimadzu UV-3600, Japan) at 233 nm. Lastly, 1 mL of fresh PBS was added to the tubes to sustain the same volume.

## RESULTS AND DISCUSSION

#### Characterization of Rheological Properties of Solutions

In this study, the solutions were prepared by adding different Metformin concentrations into the PEG and SA. The rheological properties are accepted as key parameters because of their impact on the printability of the scaffolds. Significantly, the viscosity is the most important one as it should be high enough to keep solutions in shape while printing. Also, viscosity directly affects pore size and the connection between pores. The surface tension determines the shape of the drop coming out from the nozzle. Higher surface tension makes it difficult to print one layer on top of the other, but the lower surface tension can cause a leak of the solution from the nozzle tip. Density directly connects with the viscosity of the solution, so it influences the 3D printing process [20]. The density, viscosity, and surface tension of the solutions were investigated to determine the rheological properties (Table 1). As seen in Table 1, there was a slight difference between the density values of SA/PEG and Metformin-loaded solutions. SA/PEG solutions had the most significant surface tension, but the surface tension of drug-loaded solutions decreased gradually with the increased amount of the drug. Viscosity values, on the other hand, decreased insignificantly with increasing drug concentrations.

#### Fourier Transform Infrared Spectroscopy (FTIR)

FTIR analysis was done to identify the molecular and chemical structure of the scaffolds. The analysis results for Metformin, SA, PEG, SA/PEG scaffolds, and Metformin-loaded SA/PEG scaffolds have shown in Figure 1. The infrared spectra of Metformin (Figure 1a) show the N-H stretching and bending vibrations of the primary amine group in order of 3147 and 1574  $\text{cm}^{-1}$ . At 1621  $\text{cm}^{-1}$  there are N-H bending, C-N stretching, and C=O stretching bands.  $\text{CH}_3$  asymmetric bending, C-H bending, and the

**Table 1.** Physical properties of the solutions

Solutions	Density ( $\text{g}/\text{cm}^3$ )	Surface Tension ( $\text{mN}/\text{m}$ )	Viscosity ( $\text{mPa}\cdot\text{s}$ )
SA/PEG	1.05±0.04	79.01±2.284	2644±3.183
SA/PEG/0.5MET	1.01±0.02	74.94±3.761	2640±2.047
SA/PEG/2MET	1.02±0.02	71.35±2.125	2632±5.972

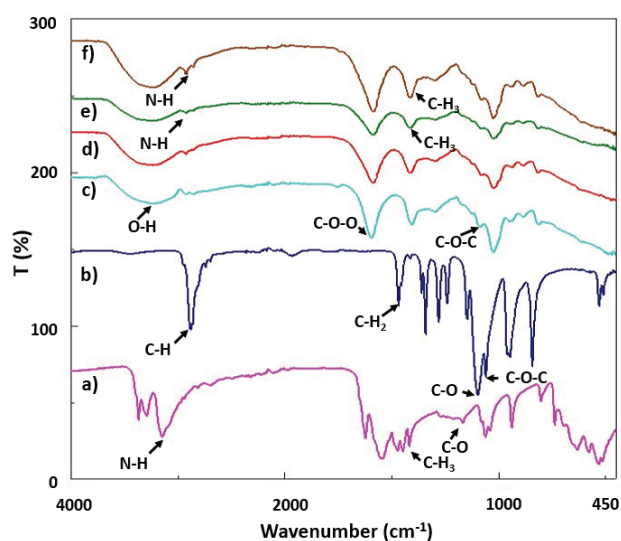


**Figure 1.** FTIR spectrums of Metformin (a), PEG (b), SA (c), SA/PEG (d), SA/PEG/0.5MET (e), SA/PEG/2MET (f).

$\text{CH}_3$  symmetrical bending vibration can be observed at 1472, 1445, and 1417  $\text{cm}^{-1}$ , respectively. Also, at 1166  $\text{cm}^{-1}$  C=O tension band was seen [21]. The spectra of the pure PEG (Figure 1b) show stretching bands of C-H, C-O of alcohol, C-O-C of ether at 2900, 1250, and 1100-1060  $\text{cm}^{-1}$ , respectively [22]. Also, the bending peak of C-H was observed at 1454  $\text{cm}^{-1}$  [23]. The spectra of pure SA (Figure 1c) show the stretching peaks of O-H, symmetric -COO-, asymmetric -COO- and -C-O-C- vibration at 3228, 1419, 1593, and 1078  $\text{cm}^{-1}$ , respectively [24]. The spectra of SA/PEG and Metformin-loaded scaffolds were similar to the spectra of SA due to the higher SA ratio in the solution. Because of the low drug ratio in Metformin-loaded scaffolds, very sharp peaks were not observed in the spectrum. However, increasing drug concentrations caused sharper peaks but there were no significant differences between SA/PEG and drug-loaded scaffolds. The peaks were shifted in Metformin-loaded scaffolds. For Metformin characteristic N-H bending peak was at 3147  $\text{cm}^{-1}$  but for 0.5 and 2 wt.% Metformin-loaded scaffolds peaks were observed at 2921 and 2919  $\text{cm}^{-1}$ , respectively. Also,  $\text{CH}_3$  symmetrical bending vibration was observed at 1415 and 1417  $\text{cm}^{-1}$  for 0.5 and 2 wt.% Metformin-loaded scaffolds. The characteristic peaks of SA, PEG, and Metformin were observed together in Metformin-loaded SA/PEG scaffolds. As a result, it can be said that drug encapsulation is achieved.

### SEM Morphological and Pore Size Analysis

Porosity and pore size is one of the most important factors affecting drug release in 3D printed scaffolds. Scaffolds should have ideal pore sizes and interconnected pores to allow nutrient flow, cell growth, and migration [25]. Also, in drug delivery systems like mesoporous nanoparticles, pore size is an important parameter for both drug loading and

drug release [26]. Different pore sizes are required for the interactions of different cell types [27]. 3D scaffolds with a pore size of 200–250  $\mu\text{m}$  show optimal proliferation for fibroblast cells [28]. In scaffolds, higher nutrient transport can be obtained with higher porosity only this causes poor mechanical strength as a result of reduced density [29]. In contrast, small pores cause limited cell migration around the scaffold [25].

In this study, SEM images and the pore size histograms were used to determine the surface morphology and the average pore sizes of the scaffolds. According to the studies, the scaffolds with pore sizes lower than 300  $\mu\text{m}$  provide sufficient permeability [30]. As shown in Figure 2, the average pore size of the SA/PEG scaffold was  $236.14 \pm 18.999 \mu\text{m}$ . Pore sizes for SA/PEG/0.5MET and SA/PEG/2MET were  $255.28 \pm 14.168$  and  $318.83 \pm 13.038 \mu\text{m}$ , respectively. The histograms show that the addition of Metformin has increased the average pore sizes, but still, there were no significant differences between scaffold morphologies. Samadzadeh et al. produced pure PLGA and Metformin-loaded PLGA nanofibers and found that Metformin addition slightly increase the fiber diameter in Metformin-loaded fibers [31].

### DSC Thermograms

DSC was done to examine the thermal properties of the scaffolds. SA is an almost amorphous polymer. SA shows an endothermic peak  $\sim 81^\circ\text{C}$ , which is a result of the evaporation of hydration water molecules, and an exothermic peak  $\sim 220^\circ\text{C}$  shows the oxidative degradation of SA [32, 33]. PEG shows an endothermic peak around 67-66 $^\circ\text{C}$  [34]. Due to the crystalline structure of Metformin a sharp endothermic peak at  $\sim 232^\circ\text{C}$  [35]. Figure 3 represents the DSC thermograms of SA/PEG and Metformin-loaded scaffolds. The thermogram of SA/PEG showed that PEG addition to the SA decreased the  $T_g$  value  $\sim 75^\circ\text{C}$ , but it increased the  $T_m$  value to  $240^\circ\text{C}$ . Metformin in different concentrations shifted the peak  $T_g$  peak  $\sim 65^\circ\text{C}$ . However, it didn't have a significant impact on the thermal behaviour of the scaffold. Previous studies have also shown that the addition of Metformin was shifted the peaks of unloaded microparticles, but sharp peaks of Metformin are not observed in thermograms. In addition, as a result of the interaction of electrostatic forces between Metformin and the polymer, it was concluded that the drug was dissolved in the matrix and encapsulation took place [35].

### Tensile Properties of Engineered Scaffolds

Mechanical properties of the SA/PEG, 0.5 and 2 wt.% Metformin-loaded SA/PEG scaffolds were analysed with the tensile tests. SA is a polysaccharide-based polymer, and they are known for its poor mechanical strength [36]. PEG is a type of plasticizer, and it decreases the tensile strength of the SA [37]. However, the mechanical properties of these scaffolds have been upgraded by blending with other polymers or crosslinking methods [36]. Table 2 shows the

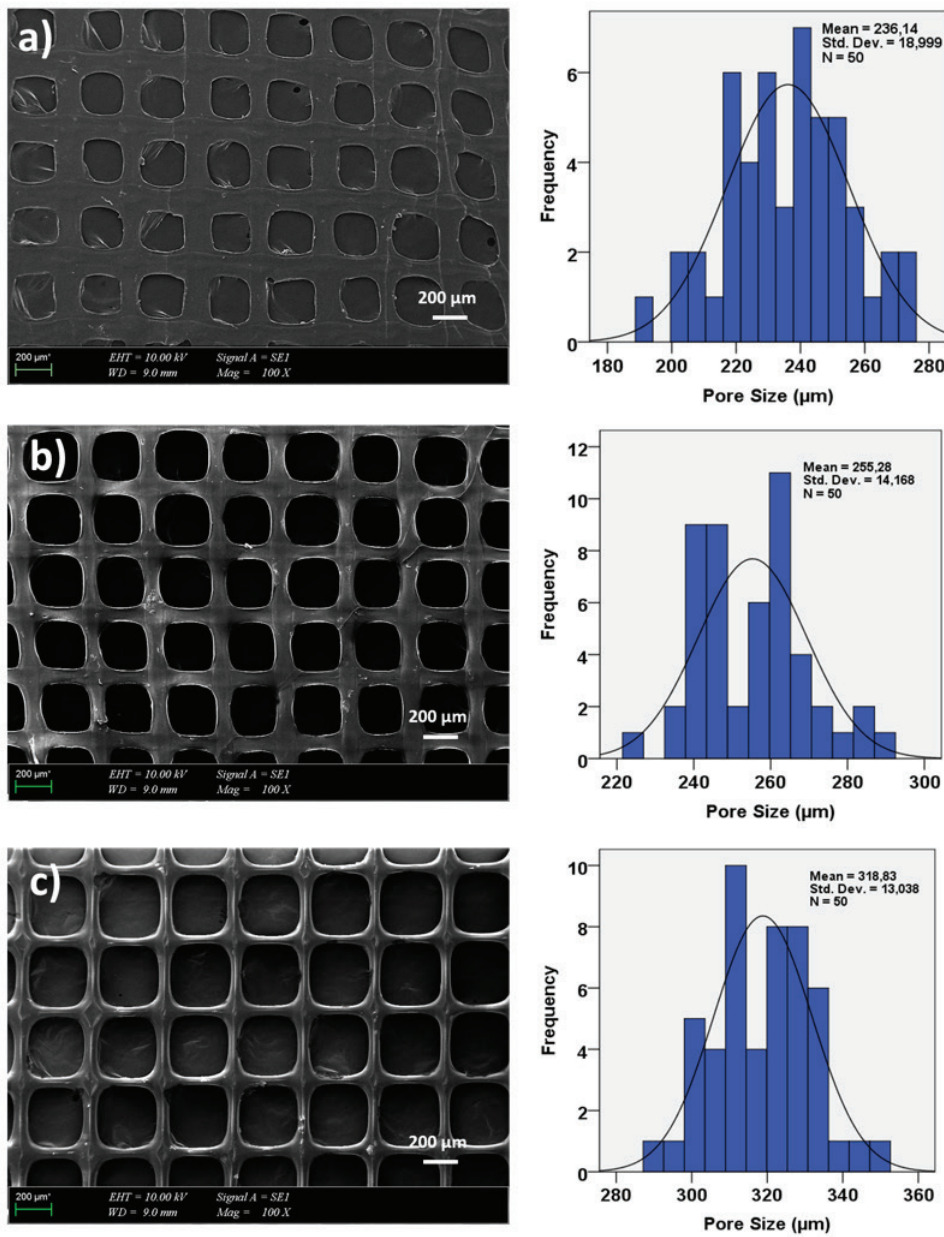


Figure 2. SEM images and pore size histograms of the SA/PEG(a), SA/PEG/0.5MET (b), SA/PEG/2MET (c) scaffolds.

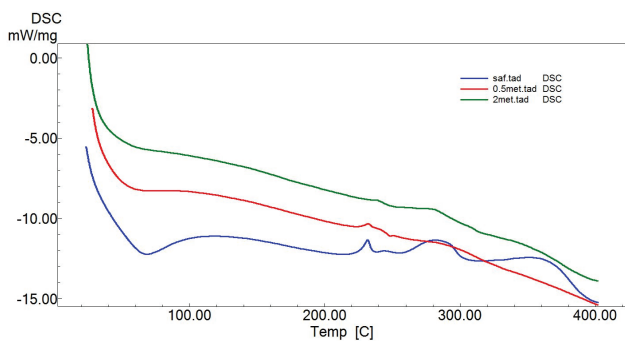


Figure 3. DSC thermogram of the 3D printed scaffolds.

tensile strength and elongation at break values for each scaffold. The tensile strength of the scaffolds varied between 4.557 and 7.048 MPa. In general, Metformin addition to the scaffolds has increased the tensile strength of the scaffolds from 4.557 to 7.048 MPa for 0.5MET and 6.163 MPa for 2MET but increasing concentrations of the drug decreased the tensile strength. The elongation of Metformin-loaded scaffolds was smaller when compared with the SA/PEG scaffold. Furthermore, the elongation decreased with the increasing drug concentration. However, Zhu et al.'s study showed Metformin decreased both the elongation and the tensile strength of PCL/CS nanofibrous membranes from

**Table 2.** Mechanical properties of the scaffolds

Scaffolds	Tensile strength (MPa)	Strain at break (%)
SA/PEG	4.557±0.028	7.120±1.028
SA/PEG/0.5MET	7.048±0.191	7.104±2.130
SA/PEG/2MET	6.163±3.145	6.824±1.315

5.4±1.0 to 4.7±0.7 and 5.1±0.2 to 4.5±0.4, respectively [38]. Overall, there were no significant changes between SA/PEG scaffold and drug-loaded scaffolds. Ebrahimi et al. produced PCL/PVA scaffolds containing different concentrations of Metformin (0, 1, 5, 10, and 15 wt.%) and showed that increased Metformin concentrations did not significantly affect the tensile strength of the scaffolds [39].

### In Vitro Drug Release Test

Drug release studies were performed by using 0.5 and 2 wt.% Metformin-loaded SA/PEG scaffolds. Figure 4a shows the UV absorbance spectra of Metformin in different concentrations (4, 6, 8, 10, 12, and 14 µg/mL). For the quantitative determination of drug release, a linear standard

calibration curve was created using the absorbance values of Metformin ( $R^2 = 0.99$ ) at 233 nm (Figure 4b). In this study, drug release from Metformin-loaded scaffolds was investigated in a neutral environment at 37 °C for 24 hours. Because of the high water-solubility of SA and PEG, the scaffolds showed a fast release of the drug in the first 30 minutes, but there were differences between 0.5 and 2 wt.% Met-loaded scaffolds (Figure 4c). The first 5-hour drug release of 0.5 wt.% Met-loaded scaffolds were 53.45, 61.34, 64.64, 67.00, 69.11, 70.94, and 75.84%. These rates were 32.73, 62.83, 75.43, 82.26, 87.47, 90.69 and 94.18% for the 2 wt.% Metformin-loaded scaffolds. In 12 hours, more than 97% of the drug for both scaffolds was released, and it reached 100% in 24 hours. Das et al. produced 5% (w/v) SA beads, which were cross-linked with 5%  $\text{CaCl}_2$ , beads released more than 50% of the drug in the first 4 hours and it reached 100% in 6 hours. Increasing SA concentrations and the type of crosslinking agents provide a more sustained release of the drug. Crosslinking with  $\text{CaCl}_2$  creates a tight junction between the guluronic acid residues and result in delayed degradation of the SA in PBS solution at pH 7.4 [40]. Also, the increased drug content in the scaffolds caused a faster release of the drug. Previous studies indicated that increasing solution viscosity reduces polymer

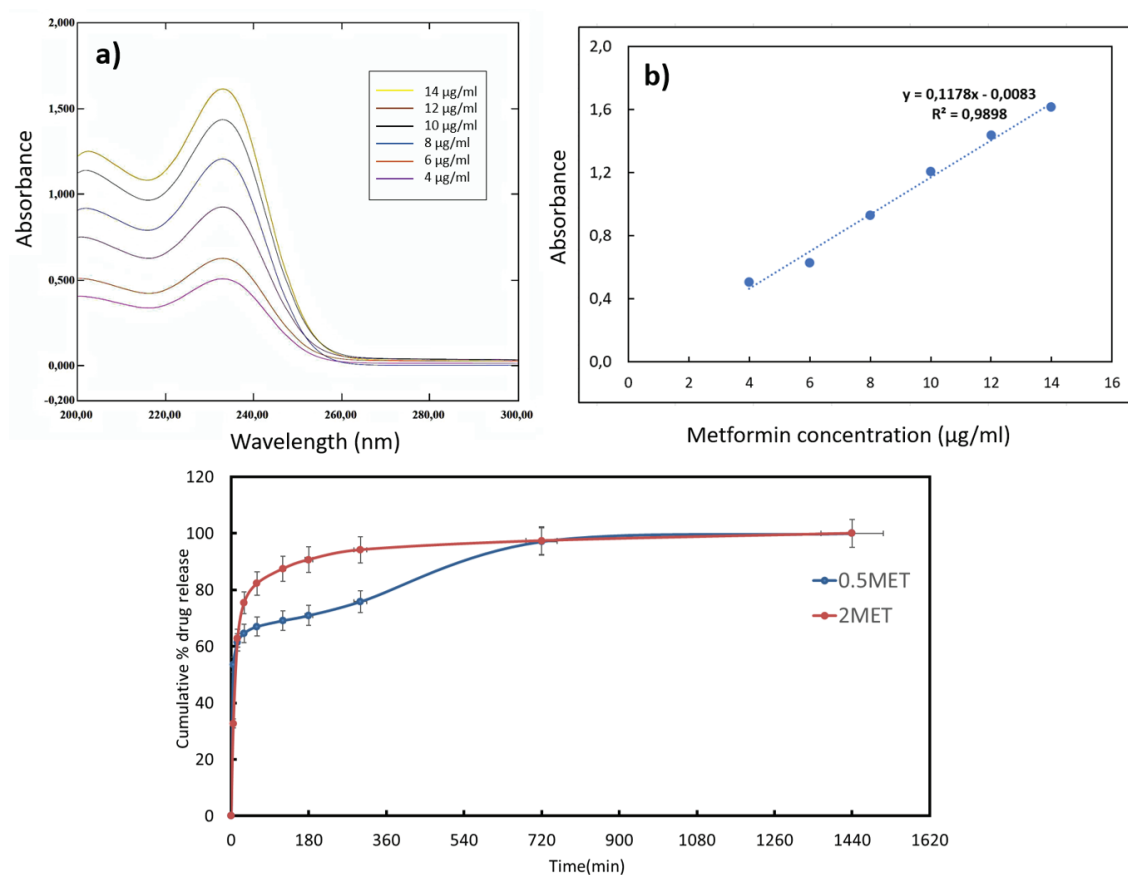


**Figure 4.** UV absorbance spectra of Metformin (a), the calibration curve for Metformin at 233 nm (b), and In-vitro release studies of the 0.5MET and 2MET scaffolds.

erosion and drug release. This shows there is a direct effect of the drug/polymer ratio of the solution on the release kinetics of the drug [41]. Sriamornsak et al. investigated the effect of drug loading method and drug content on the drug release from calcium pectinate gel beads and found that higher drug content causes faster drug release, which may be the effect of decreased polymer-to-drug ratio [42].

## CONCLUSION

In this study, Metformin-loaded 3D printed scaffolds were produced for an alternative drug delivery application in the treatment of T2DM. SA/PEG scaffolds loaded with different concentrations of Metformin (0.5 and 2 wt.%) were prepared by adding 9 wt.% of SA to 3 wt.% of PEG. SA was chosen before its excellent biocompatibility and biodegradability. Metformin, an oral antidiabetic drug, was preferred because it is a drug with proven effectiveness for T2DM. When the SEM images of the scaffolds were examined, the desired porosity was obtained with the 3D printing method. Except for the SA/PEG/2MET scaffold, the average pore size of the other scaffolds was below 300  $\mu\text{m}$ . All the scaffolds had desired mechanical properties, but Metformin-loaded scaffolds showed better resistance to the break than the SA/PEG scaffolds. Both 0.5 and 2 wt.% Metformin-loaded scaffolds, drug release occurred rapidly in the first 30 minutes due to the high water-solubility of the polymers used in the scaffolds, but the release lasted up to 24 hours. As expected, drug release from the scaffold containing 2 wt.% Metformin was faster than that of 0.5 wt.%. This may be due to increased drug concentration in the polymer matrix and/or decreased viscosity of the solution. According to the results obtained in this study, Metformin-loaded 3D-printed scaffolds have promising potential for oral administration of anti-diabetics used in the treatment of T2DM.

## AUTHORSHIP CONTRIBUTIONS

Authors equally contributed to this work.

## DATA AVAILABILITY STATEMENT

The authors confirm that the data that supports the findings of this study are available within the article. Raw data that support the finding of this study are available from the corresponding author, upon reasonable request.

## CONFLICT OF INTEREST

The author declared no potential conflicts of interest with respect to the research, authorship, and/or publication of this article.

## ETHICS

There are no ethical issues with the publication of this manuscript.

## REFERENCES

- [1] Chatterjee S, Khunti K, Davies MJ. Type 2 diabetes. *Lancet* 2017;389:2239–2251. [\[CrossRef\]](#)
- [2] International Diabetes Federation. IDF Diabetes Atlas. 9th ed. Diabetes Atlas <http://www.diabetesatlas.org/> 2019.
- [3] Turner RC, Cull CA, Frighi V, Holman RR, UK Prospective Diabetes Study (UKPDS) Group. Glycemic control with diet, sulfonylurea, metformin, or insulin in patients with type 2 diabetes mellitus: progressive requirement for multiple therapies (UKPDS 49). *JAMA* 1999;281:2005v2012. [\[CrossRef\]](#)
- [4] Stein SA, Lamos EM, Davis SN. A review of the efficacy and safety of oral antidiabetic drugs. *Expert Opin Drug Saf* 2013;12:153–175. [\[CrossRef\]](#)
- [5] Foretz M, Guigas B, Viollet B. Understanding the glucoregulatory mechanisms of metformin in type 2 diabetes mellitus. *Nat Rev Endocrinol* 2019;15:569–589. [\[CrossRef\]](#)
- [6] Krentz AJ, Bailey CJ. Oral antidiabetic agents. *Drugs* 2005;65:385–411. [\[CrossRef\]](#)
- [7] Nasri H, Rafeian-Kopaei M. Metformin: current knowledge. *J Res Med Sci* 2014;19:658. [\[CrossRef\]](#)
- [8] Cesur S, Cam ME, Sayın FS, Su S, Harker A, Edirisinghe M, Gunduz O. Metformin-loaded polymer-based microbubbles/nanoparticles generated for the treatment of type 2 diabetes mellitus. *Langmuir* 2022;38:5040–5051. [\[CrossRef\]](#)
- [9] Berman B. 3-D printing: The new industrial revolution. *Bus Horiz* 2012;55:155–162. [\[CrossRef\]](#)
- [10] Calori IR, Braga G, de Jesus PDCC, Bi H, Tedesco AC. Polymer scaffolds as drug delivery systems. *Eur Polym J* 2020;129:109621. [\[CrossRef\]](#)
- [11] Vaezi M, Zhong G, Kalami H, Yang S. Extrusion-based 3D printing technologies for 3D scaffold engineering. In *Functional 3D Tissue Engineering Scaffolds*. Cambridge: Woodhead Publishing; 2018. p. 235–254. [\[CrossRef\]](#)
- [12] Annaji M, Ramesh S, Poudel I, Govindarajulu M, Arnold RD, Dhanasekaran M, et al. Application of extrusion-based 3d printed dosage forms in the treatment of chronic diseases. *J Pharm Sci* 2020;109:3551–3568. [\[CrossRef\]](#)
- [13] Palo M, Holländer J, Suominen J, Yliruusi J, Sandler N. 3D printed drug delivery devices: perspectives and technical challenges. *Expert Rev Med Dev* 2017;14:685–696. [\[CrossRef\]](#)
- [14] Nikolova MP, Chavali MS. Recent advances in biomaterials for 3D scaffolds: A review. *Bioact Mater* 2019;4:271–292. [\[CrossRef\]](#)
- [15] Wang Y, Wang X, Shi J, Zhu R, Zhang J, Zhang Z, et al. A biomimetic silk fibroin/sodium alginate composite scaffold for soft tissue engineering. *Sci Rep* 2016;6:1–13. [\[CrossRef\]](#)

- [16] Shen W, Hsieh YL. Biocompatible sodium alginate fibers by aqueous processing and physical crosslinking. *Carbohydr Polym* 2014;102:893–900. [CrossRef]
- [17] Wu J, Wei W, Wang LY, Su ZG, Ma GH. A thermosensitive hydrogel based on quaternized chitosan and poly (ethylene glycol) for nasal drug delivery system. *Biomaterials* 2007;28:2220–2232. [CrossRef]
- [18] Chiu YC, Larson JC, Isom Jr A, Brey EM. Generation of porous poly (ethylene glycol) hydrogels by salt leaching. *Tissue Eng Part C Methods* 2010;16:905–912. [CrossRef]
- [19] Chen BY, Jing X, Mi HY, Zhao H, Zhang WH, Peng XF, et al. Fabrication of polylactic acid/polyethylene glycol (PLA/PEG) porous scaffold by supercritical CO<sub>2</sub> foaming and particle leaching. *Polym Eng Sci* 2015;55:1339–1348. [CrossRef]
- [20] You F, Wu X, Chen X. 3D printing of porous alginate/gelatin hydrogel scaffolds and their mechanical property characterization. *Int J Polym Mater Polym Biomater* 2017;66:299–306. [CrossRef]
- [21] Cesur S, Cam ME, Sayin FS, Su S, Gunduz O. Controlled Release of Metformin Loaded Polyvinyl Alcohol (PVA) Microbubble/Nanoparticles Using Microfluidic Device for the Treatment of Type 2 Diabetes Mellitus. In *IWBBIO 2020*, May. pp. 185–193. [CrossRef]
- [22] Pramono E, Utomo SB, Wulandari V, Clegg F. FTIR studies on the effect of concentration of polyethylene glycol on polymerization of Shellac. *J Physics Conf Ser* 2016;776: 012053. [CrossRef]
- [23] Shameli K, Bin Ahmad M, Jazayeri SD, Sedaghat S, Shabanzadeh P, Jahangirian H, et al. Synthesis and characterization of polyethylene glycol mediated silver nanoparticles by the green method. *Int J Mol Sci* 2012;13:6639–6650. [CrossRef]
- [24] Cesur S, Oktar FN, Ekren N, Kilic O, Alkaya DB, Seyhan SA et al. Preparation and characterization of electrospun polylactic acid/sodium alginate/orange oyster shell composite nanofiber for biomedical application. *J Aust Ceram Soci* 2020;56:533–543. [CrossRef]
- [25] Murphy CM, O'Brien FJ. Understanding the effect of mean pore size on cell activity in collagen-glycosaminoglycan scaffolds. *Cell Adh Migr* 2010;4:377–381. [CrossRef]
- [26] Li J, Shen S, Kong F, Jiang T, Tang C, Yin C. Effects of pore size on in vitro and in vivo anticancer efficacies of mesoporous silica nanoparticles. *RSC Adv* 2018;8:24633–24640. [CrossRef]
- [27] Sultan S, Mathew AP. 3D printed scaffolds with gradient porosity based on a cellulose nanocrystal hydrogel. *Nanoscale* 2018;10:4421–4431. [CrossRef]
- [28] Choi DJ, Park SJ, Gu BK, Kim YJ, Chung S, Kim CH. Effect of the pore size in a 3D bioprinted gelatin scaffold on fibroblast proliferation. *J Ind Eng Chem* 2018;67:388–395. [CrossRef]
- [29] Egan PF. Integrated design approaches for 3D printed tissue scaffolds: Review and outlook. *Materials* 2019;12:2355. [CrossRef]
- [30] Hutmacher DW, Schantz JT, Lam CXF, Tan KC, Lim TC. State of the art and future directions of scaffold-based bone engineering from a biomaterials perspective. *J Tissue Eng Regen Med* 2007;1:245–260. [CrossRef]
- [31] Samadzadeh S, Mousazadeh H, Ghareghomi S, Dadashpour M, Babazadeh M, Zarghami N. In vitro anticancer efficacy of Metformin-loaded PLGA nanofibers towards the post-surgical therapy of lung cancer. *J Drug Deliv Sci Technol* 2021;61:102318. [CrossRef]
- [32] Swamy TM, Ramaraj B, Lee JH. Sodium alginate and its blends with starch: thermal and morphological properties. *J Appl Polym Sci* 2008;109:4075–4081. [CrossRef]
- [33] AlKhatib HS, Taha MO, Aiedeh KM, Bustanji Y, Sweileh B. Synthesis and in vitro evaluation of iron-crosslinked N-methyl and N-benzyl hydroxylated derivatives of alginate as controlled release carriers. *Eur Polym J* 2006;42:2464–2474. [CrossRef]
- [34] Barkat K, Ahmad M, Minhas MU, Khalid I, Mahmood A. Understanding mechanical characteristics of pH-responsive PEG 4000-based polymeric network for colorectal carcinoma: its acute oral toxicity study. *Polym Bull* 2020;1–27. [CrossRef]
- [35] Bouriche S, Alonso-García A, Cárceles-Rodríguez CM, Rezgui F, Fernández-Varón E. An in vivo pharmacokinetic study of metformin microparticles as an oral sustained release formulation in rabbits. *BMC Vet Res* 2021;17:1–11. [CrossRef]
- [36] Shelke NB, James R, Laurencin CT, Kumbar SG. Polysaccharide biomaterials for drug delivery and regenerative engineering. *Polym Adv Technol* 2014;25:448–460. [CrossRef]
- [37] Giyatmi G, Eka Poetri TA, Irianto H, Fransiska D, Agusman A. Effect of alginate and polyethylene glycol addition on physical and mechanical characteristics of k-carrageenan-based edible film. *Squalen Bullet Marine Fisheries Postharvest Biotechnol* 2020;15:41–51. [CrossRef]
- [38] Zhu J, Ye H, Deng D, Li J, Wu Y. Electrospun metformin-loaded polycaprolactone/chitosan nanofibrous membranes as promoting guided bone regeneration membranes: Preparation and characterization of fibers, drug release, and osteogenic activity in vitro. *J Biomater Appl* 2020;34:1282–1293. [CrossRef]
- [39] Ebrahimi L, Farzin A, Ghasemi Y, Alizadeh A, Goodarzi A, Basiri A, Ai J. Metformin-loaded PCL/PVA fibrous scaffold preseeded with human endometrial stem cells for effective guided bone regeneration membranes. *ACS Biomater Sci Eng* 2020;7:222–231. [CrossRef]

- [40] Das MK, Senapati PC. Furosemide-loaded alginate microspheres prepared by ionic cross-linking technique: Morphology and release characteristics. *Indian J Pharm Sci* 2008;70:77. [\[CrossRef\]](#)
- [41] Ozoude CH, Azubuike CP, Ologunagba MO, Tonuewa SS, Igwilo CI. Formulation and development of metformin-loaded microspheres using *Khaya senegalensis* (Meliaceae) gum as co-polymer. *Future J Pharm Sci* 2020;6:1–11. [\[CrossRef\]](#)
- [42] Sriamornsak P, Nunthanid J, Cheewatanakornkool K, Manchun S. Effect of drug loading method on drug content and drug release from calcium pectinate gel beads. *AAPS Pharm Sci Tech* 2010;11:1315–1319. [\[CrossRef\]](#)